Venus' Mass Spectra Show Signs of Disequilibria in the Middle Clouds

Rakesh Mogul[1], Sanjay S. Limaye[2], M. J. Way[3,4,5]

[1] Chemistry & Biochemistry Department, California State Polytechnic University, Pomona, 3801 W. Temple Dr., Pomona, CA, USA
[2] Space Science and Engineering Center, University of Wisconsin, 1225 West Dayton Street, Madison, WI, USA
[3] NASA Goddard Institute for Space Studies, 2880 Broadway, New York, NY, USA
[4] GSFC Sellers Exoplanet Environments Collaboration, Greenbelt, MD, USA
[5] Theoretical Astrophysics, Department of Physics and Astronomy, Uppsala University, Uppsala, Sweden

***Corresponding author:** Rakesh Mogul (rmogul@cpp.edu)

Key Points:

- Mass data from the Pioneer Venus Large Probe Neutral Mass Spectrometer reveals several minor chemical species suggestive of disequilibria.
- Minor species include nitrous acid, nitric acid, ammonium, carbon monoxide, ethane, and phosphine and/or hydrogen sulfide.
- The assignments reveal a potential electron donor for anoxygenic photosynthesis (nitrite), and include the nitrogen cycle members.

Abstract

We present a re-examination of published mass spectral data obtained from the Pioneer Venus Large Probe Neutral Mass Spectrometer (51.3 km). Our interpretations support the presence of minor chemical species that are suggestive of disequilibria in Venus' middle clouds. Assignments to the data include nitrous acid, nitric acid, ammonium, carbon monoxide, ethane, phosphine and/or overlapping hydrogen sulfide, hydrochloric acid, and potentially benzene, methane, ethene, and chlorous acid. Chemical assignments were predicated upon matching parent ions to fragmentation products, and atomic elements to parent ions. The data reveal parent ions at varying oxidation states, implying the presence of reducing power in the clouds. Interestingly, when considering the potential habitability of Venus' clouds, the assignments reveal a potential electron donor for anoxygenic photosynthesis (nitrite), and all major constituents of the nitrogen cycle (nitrate, nitrite, possibly ammonium, N_2). Our mass assignments illuminate the potential for chemistries yet to be discovered on Venus.

Plain Language Summary

We re-examined data obtained from the Pioneer Venus Large Probe Neutral Mass Spectrometer. Our results reveal the likely presence of several minor chemical species such as nitrite, nitrate, ethane, and possibly ammonium and phosphine. The total chemical assignments to the mass data suggest that Venus' clouds are not at equilibrium. These results illuminate the potential for chemistries yet to be discovered. Further, when considering the potential habitability of Venus' clouds, our work reveals chemicals that could contribute to anoxygenic photosynthesis (nitrite) and the nitrogen cycle (nitrate, nitrite, possibly ammonium, and N_2).

1. Introduction

Venus' clouds harbor a number of putative minor chemical species that may illuminate chemistries yet to be discovered. Among these previously proposed species are ammonia, oxygen, hydrogen, methane, and ethene (*Smirnova and Kuz'min*, 1974; *Surkov*, 1977; *Oyama et al.*, 1980; *Kumar et al.*, 1981; *Moroz*, 1981; *Pollack et al.*, 1993). More recently, *Greaves et al.* (2020) reported on the possible detection of phosphine (at 1.123 mm), which has spurred debate within the community on the possible presence of such molecules within Venus' atmosphere. In this light, we sought to examine available in-situ data for any related signatures for phosphine and other minor species. For this report, we focused on data obtained from the Pioneer Venus (PV) Large Probe Neutral Mass Spectrometer (LNMS), which sampled the atmosphere during descent below ~64 km (*Hoffman et al.*, 1979a). Given recent interest in the potential habitability of the lower/middle clouds (*Limaye et al.*, 2018; *Greaves et al.*, 2020; *Seager et al.*, 2020), we concentrated on data obtained at an altitude of 51.3 km that included counts for masses between 1 – 208 amu, and was previously published in identical tables in *Hoffman et al.* (1980a) and *Hoffman et al.* (1980b).

Review of the literature related to the LNMS reveals a significant focus on the *major* Venus atmospheric constituents (*e.g.*, noble gases, CO_2, N_2, & SO_2), with less attention given to the identification of minor species, apart from methane and water (*Hoffman et al.*, 1979a; *Hoffman et al.*, 1979b, c; *Hoffman et al.*, 1980a; *Hoffman et al.*, 1980b; *Hoffman et al.*, 1980c; *Donahue et al.*, 1982; *Donahue and Hodges*, 1992, 1993). The LNMS data were additionally discussed by *Von Zahn and Moroz* (1985), as part of the Venus International Reference Atmosphere Model (*Kliore et al.*, 1985). A comprehensive but not exhaustive list from Venus observations (space and ground) can be found in *Johnson and de Oliveira* (2019). Beyond these studies, there is limited information on the assignment of minor chemicals, and associated fragmentation products, across the range of masses in the LNMS data.

In this study, we present an agnostic interpretation of the published LNMS mass data. Our chemical assignments both match and expand upon those from *Hoffman et al.* (1979b) and

Hoffman et al. (1980a). In total, the assignments support the presence of a number of molecular species in potential disequilibrium, including nitrous acid (HNO_2), ammonium (NH_4^+), carbon monoxide (CO), ethane (C_2H_6), and potentially phosphine (PH_3), benzene (C_6H_6), methane (CH_4), ethene (C_2H_4), and chlorous acid ($HClO_2$). While these chemicals hint at chemistries yet to be discovered, further work is required to evaluate the veracity of the assignments through analysis of the remaining PV LNMS data across all altitudes.

2. Data and Methods

The PV LNMS contained a magnetic sector-field mass analyzer, gas inlets and pumping system for sample acquisition, simultaneously examining low (1-15 amu) and high mass (15-208 amu) channels, and a microprocessor which peak-stepped across pre-selected masses during descent (*Hoffman et al.*, 1980b). The gas inlets were opened within the upper atmosphere (~62 km) after deployment of the parachute and release of the heat shield. Gases were sampled through a pair of 6 cm metal tubes (3.2 mm diameter), and passed on to the ion source (impact enegies of 70, 30, or 22 eV), while maintaining a constant pressure. Per *Hoffman et al.* (1980b), the constant pressure of the ion source preserved a dynamic range of ">6 decades" across the tremendous changes in atmospheric pressure towards the surface (~10^{-2}-10^2 bars). In total, 51 spectra were obtained every 1.2 km on average.

Sensitivities of the LNMS were reported at "1 part per million (ppm) relative to CO_2" (*Hoffman et al.*, 1980b). In *Hoffman et al.* (1980a) and *Hoffman et al.* (1979b), upper counts for CO_2 were reported as ~1.8×10^6 (*e.g.*, CO_2), and abundances were estimated using counts as low as 5-7 (*e.g.*, ^{18}OH, SO_2, & ^{37}Cl). In *Hoffman et al.* (1980b), an example resolving power ($m/\Delta m$) for the LNMS was stated as ≥440 (10 percent valley); while *Hoffman et al.* (1980a) demonstrated a minimum resolving power (RP) of ≥702 through assignment of ^{40}Ar and C_3H_4. To obtain an upper estimate of the RP, at least for the minimum purpose of chemical assignments, we compared the apparent resolving powers needed to separate the mass triplet of 19.007, 18.998, 18.987 amu (which amounted to RPs = 2112 and 1727, respectively; **Table**

S1). At these masses, per our understanding, *Hoffman et al.* (1980a) disentangled the counts at 19.007 and 18.998 amu to obtain abundances of $^{18}OH^+$ and HDO^+, and assigned $^{38}Ar^{2+}$ to 18.987 amu. In this context, we used an effective RP of ≤1727 as an upper limit to the resolving power.

To gauge the accuracy of the calibration of the LNMS, we compared the expected masses of the presumed expected species at the pre-selected positions (the actual identities of the pre-selected species were not available). Comparisons were conducted across 11 different non-controversial parent ions, which spanned 15-86 amu. This included CO_2^+, $^{13}CO_2^+$, $^{14}N_2^+$, $^{20}Ne^+$, $^{21}Ne^+$, $^{22}Ne^+$, $^{32}SO_2^+$, $^{36}Ar^+$, $^{37}Cl^+$, $^{40}Ar^+$, and $^{86}Kr^+$. Expected masses were calculated using exact amu values obtained from the CRC Handbook of Chemistry and Physics (*Haynes*, 2016). Differences between measured (LNMS) and expected (CRC) amu values (Δamu; absolute value) ranged from 0.000-0.003 amu, and averaged 0.001 ± 0.001 amu (standard deviation). We've interpreted this as an indication of excellent calibration, with no significant drift across 15-86 amu.

Under these constraints, therefore, we leveraged the high-resolution LNMS mass data to identify minor species, where assignments were predicated upon (A) the identification of associated fragmentation products, (B) identification of isotopologues (if so possible), and (C) accounting of all observed atomic species to respective parent ions. Given sufficient resolution, identities were parsed using a maximum difference between measured and expected masses (Δamu) of ≤0.006 amu, referred to herein as Δamu_{max}. This value provided a conservative 2-fold higher allowance above the maximum drift in accuracy noted above (Δamu = 0.003 amu). Above 86 amu, no major assignments were made; barring the calibrants of ^{134}Xe and ^{136}Xe, and other Xe isotopes.

3. Results

Our analysis of the LNMS mass data (summarized in **Tables 1, S1**, & **S2**) show evidence of hydrocarbons, nitrogen species, and sulfur species in differing oxidation and protonation states. More surprisingly, the data show the presence of atomic phosphorous ($^{31}P^+$), which is

presumably a fragment from a neutral phosphorous-containing gas. Under the described constraints, the combined data are suggestive of phosphine and elemental sulfur being constituents of the lower clouds. The LNMS data also revealed the whole suite of CHNOPS elements, and additionally B, Cl, and Se (**Figure S1A**); however, no parent ions for B^+ were identified, and elemental selenium tentatively served as a parent source. Across the list of masses, isotopologues containing ^2H (D), ^{13}C, ^{15}N, ^{18}O, or ^{34}S were also observed; as were elemental isotopes of ^{20}Ne, ^{21}Ne, ^{22}Ne, $^{32}SO_2$, ^{36}Ar, ^{38}Ar, ^{40}Ar, ^{37}Cl, ^{78}Se, and ^{80}Se. The most abundant parent ion was CO_2^+ with counts of 1,769,472. Additional polyatomic ions included COS^+ and SO_2^+; while diatomic ions included N_2^+, O_2^+, CO^+. Lastly, water and several monoprotic acids were assigned including nitrous acid (HNO_2), nitric acid (HNO_3), hydrochloric acid (HCl and $H^{37}Cl$), and possibly hydrofluoric acid (HF), chlorous acid ($HClO_2$), and hydrogen cyanide (HCN).

For all parent species, mass and count data from related chemical fragments were binned and plotted against reference mass spectra obtained from the NIST Chemistry WebBook (https://webbook.nist.gov/chemistry/) (*Wallace*, 2020), MassBank Europe (https://massbank.eu/MassBank/), or from published reports. Described below are fragmentation patterns and isotopologues (if so present) for ethane (C_2H_6), methane (CH_4), ethene (C_2H_4), benzene (C_6H_6), phosphine (PH_3), ammonium (NH_4^+), HNO_2 and HNO_3 (H_xNO_y), oxysulfur species (H_xSO_y), and HCl. As an internal reference, **Figure 1A** displays the remarkably similar fragmentation patterns for carbon dioxide (CO_2; ~$1.8x10^6$ counts) across the LNMS (which included both mass channels) and NIST reference spectrum. Yields for CO^+, O^+, and C^+ were higher in the LNMS, which was suggestive of alterations in fragmentation yields (*Hoffman et al.*, 1979b) and/or enrichment from atmospheric CO. Indeed, fragmentation yields for methane (CH_4; ~$4.0x10^4$ counts) were not identical to the NIST reference (**Figure S1B**), with the LNMS data showing a ~18% decrease in yield of CH_3^+, despite the potential for mixing from ^+NH. Hence, for these analyses, assignments relied upon fragmentation trends and Δamu, with comparison of yields reserved for higher abundance species.

Table 1. Assignment of parent species for the LNMS mass data collected at 51.3 km.

amu	count	identity[a]	expected amu	Δamu[b]	amu	count	identity[a]	expected amu	Δamu[b]
2.016	22016	H_2	2.014102	0.002	35.005	12	PH_2D	35.003659	0.001
16.031	39936	CH_4	16.031300	0.000			HDS	34.993998	*0.011*
17.026	244	NH_3	17.026549	0.001	35.981	704	HCl	35.976678	0.004
		$^{13}CH_4$	17.034655	*0.009*	37.968	152	$H^{37}Cl$	37.973728	0.006
18.010	1088	H_2O	18.010650	0.001	40.029	80	C_3H_4	40.031300	0.002
18.034	66	NH_4	18.034374	0.000	43.991	1769472	CO_2	43.990000	0.001
20.006	112	*HF*	20.006228	0.000	44.991	21504	$^{13}CO_2$	44.993355	0.002
20.015	30	$H_2{}^{18}O$	20.014810	0.000	44.991	7936	$CO^{18}O$	44.993355	0.002
		D_2O	20.023204	*0.008*	47.000	94	HNO_2	47.000899	0.001
27.010	102	*HCN*	27.010899	0.001	59.966	1	COS	59.967071	0.001
27.988	335053	CO[c]	27.995000	0.007	62.994	1	HNO_3	62.995899	0.002
28.012	159744	N_2	28.012130	0.000	63.962	5	SO_2	63.962071	0.000
28.032	122880	C_2H_4[d]	28.031300	0.001	65.961	1	$^{34}SO_2$[c]	65.957867	0.003
28.997	7040	^{13}CO	28.998355	0.001	67.964	6272	*$HClO_2$*	67.966678	0.003
29.997	754	$C^{18}O$	29.999160	0.002	78.053	16	C_6H_6	78.046950	0.006
30.046	208	C_2H_6	30.046950	0.001	80.947	1	*NSCl*	80.943998	0.003
31.990	320	O_2	31.990000	0.000					
33.992	19	PH_3	33.997382	0.005					
		H_2S	33.987721	0.004					
34.005	21	H_2O_2	34.005650	0.001					

(a) italics: tentative assignment
(b) italics: Δamu > Δamu_{max}
(c) maximum theoretical counts
(d) potential parent and/or fragment ion

3.1 Low-Mass Organics

Mass data and assignments for methane (CH_4), ethane (C_2H_6), ethene (C_2H_4), benzene (C_6H_6), and related fragments are provided in **Table S1**. Fragmentation of CH_4 (**Figure S1B**) yielded CH_3^+ in reduced yields, when compared to the NIST spectrum, yet followed the same general trend with the parent ion (CH_4^+) having the highest relative intensity (base peak). Atomic carbon was enriched at 861% (normalized to the base peak) as expected due to tremendous input from CO_2. Ionization and fragmentation of ethane yielded 5 of the 7 signature lines from the NIST spectrum, with the two missing masses likely below the LNMS limit of detection. Present in the data were masses for $C_2H_6^+$ (M^+) and fragments representing successive hydrogen losses to yield $C_2H_5^+$ ($[M-H]^+$), $C_2H_4^+$ ($[M-2H]^+$), $C_2H_3^+$ ($[M-3H]^+$), and $C_2H_2^+$ ($[M-4H]^+$).

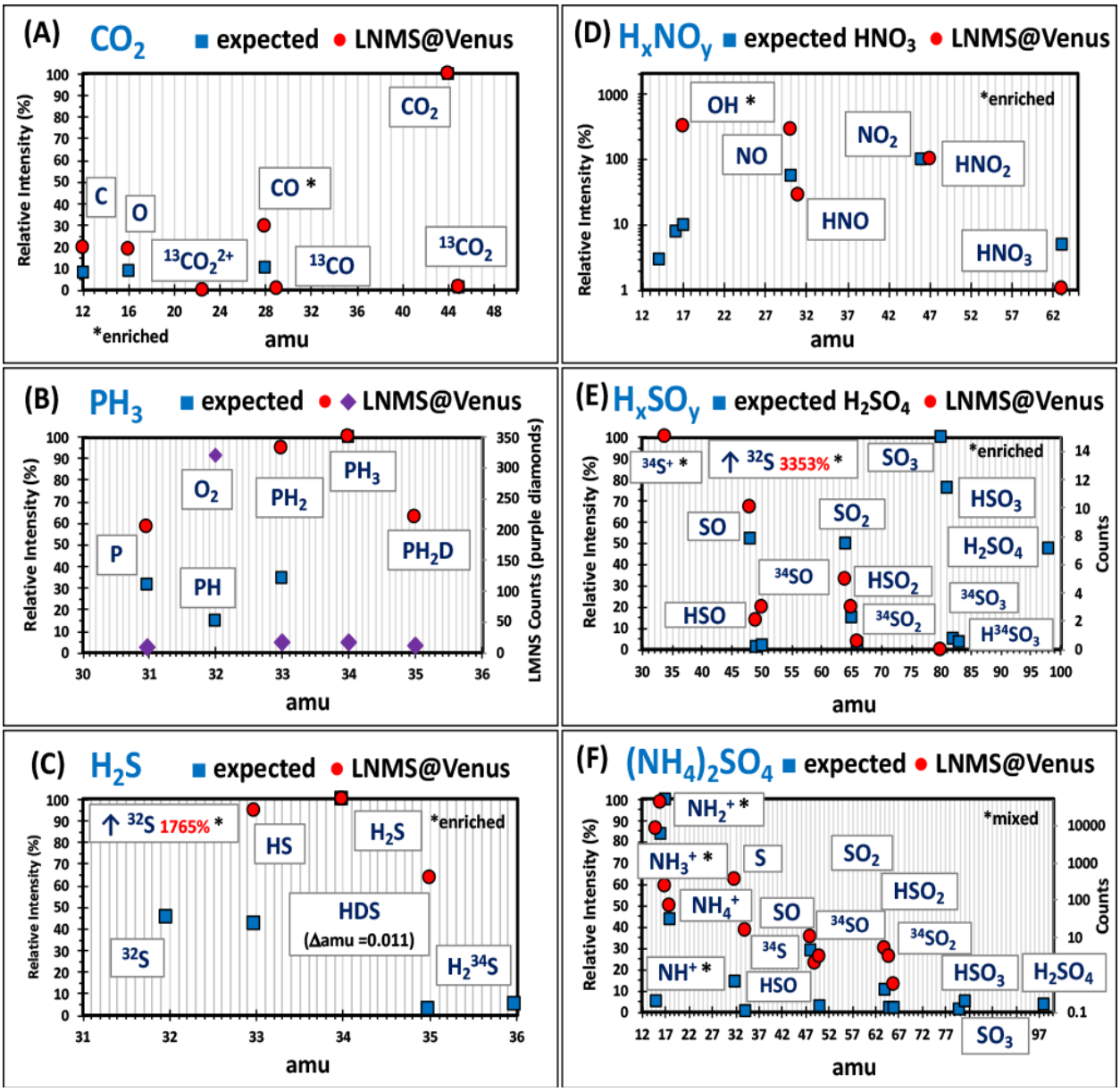

Figure 1. Comparison of fragmentation patterns from the LNMS data (circles, red) and reference spectra from the NIST Chemistry WebBook or published reports (squares, blue); selected chemicals included (A) carbon dioxide, (B) phosphine, (C) hydrogen sulfide, (D) nitrous and nitric acids (H_xNO_y), (E) sulfate/sulfuric acid fragments (H_xSO_y), and (F) ammonium sulfate. Reference spectra were plotted as relative abundances, as were the LNMS data for CO_2, PH_3, H_2S, and H_xNO_y; however, for H_xSO_y, counts were plotted on the secondary y-axis, and counts for $(NH_4)_2SO_4$ were plotted on the secondary y-axis using a log scale. For PH_3, the respective counts for PH_3^+, PH_2^+, O_2^+, and P^+ are additionally provided (diamonds, secondary y-axis). Abundance of off-scale atomic sulfur from LNMS data is noted for H_2S and H_xSO_y fragments.

While fragmentation patterns for ethane followed the general trend of the NIST reference, the intensities for $C_2H_4^+$ were incredibly enriched (as indicated by the log-scale on the secondary y-axis in **Figure S1C**), suggesting the presence of ethene (C_2H_4) and/or mixing with N_2 (which is reasonable considering the high counts of ~$5x10^5$ for N_2 and upper RP value of 1402). Fragmentation of ethene (**Figure S1D**) yielded products with the same mass as those from ethane ($C_2H_3^+$ and $C_2H_2^+$). However, the higher relative yield for the $C_2H_2^+$ fragment was suggestive of enrichment; possibly from ethyne (C_2H_2). Though, the major fragmentation product for ethyne (C_2H^+; 25.007825 amu) could not be observed as the mass value was not sampled by the LNMS.

For benzene (**Figure S1E**), the LNMS data contained masses corresponding to $C_6H_6^+$ (M^+, counts = 16) and $C_6H_5^+$ ($[M-H]^+$, counts = 2), which represented the 2 major species in the NIST reference spectrum. Fragmentation patterns were similar, though yields were slightly lower than expected. The next major fragments between 50-52 amu could not be observed as the mass values were not measured by the LNMS. Additionally, while *Hoffman et al.* (1980a) explicitly assigned C_3H_4 (propyne or allene) in the LNMS data (**Figure S1F**), the major fragmentation product $C_3H_3^+$ (39.023475 amu) could not be observed, as the mass value again was not measured by the LNMS. The potential for organic contamination is discussed in the supplemental section.

3.2 Phosphine and/or Hydrogen Sulfide

Mass data and assignments for phosphine (PH_3) or hydrogen sulfide (H_2S) and associated fragments and isotopologues are provided in **Table S1**. Comparison of the exact masses for $^+PH_3$ and H_2S^+, and $^+PH_2$ and HS^+, revealed Δm values of 0.009661 that respectively translated to minimum resolving powers of 3519 and 3414 (required for full separation), which are likely outside of the LNMS capabilities. By this assessment, the parent ion and first

fragmentation product ($[M-H]^+$) could not be unambiguously assigned to the parent gases of PH_3 or H_2S.

Rather, in an attempt to assign chemical identities, we followed a step-wise rationale that provided equal probability to PH_3 and H_2S:

1. Both atomic phosphorous and sulfur were unambiguously assigned.

2. The mass at **33.992 amu** represents $^+PH_3$ (33.997382 amu), H_2S^+ (33.987721 amu), or a composite mass containing roughly equal abundances of $^+PH_3$ and H_2S^+. [Theoretical composite mass of M^+: **33.992 amu** ≈ *33.9925516* amu = 50%*33.997382 amu $^+PH_3$ + 50%*33.987721 amu H_2S^+.]

3. The mass at **32.985 amu** represents $^+PH_2$ (32.989557 amu), HS^+ (32.979896 amu), or a composite mass containing roughly equal abundances of $^+PH_2$ and HS^+. [Theoretical composite mass for $[M-H]^+$: **32.985 amu** = *32.9847266* amu = 50%*32.989557 amu $^+PH_2$ + 50%*32.979896 amu ^+SH.]

4. The fragment of ^+PH (31.981732 amu) was not available for detection since (A) it was thoroughly masked by $^+O_2$ (**31.990 amu**, measured; counts = 320), which was ~17-fold higher in intensity than the $^+PH_3$ parent ion (counts = 19), which is the base peak in the NIST reference spectrum (see diamonds in **Figure 1B**), (B) separation of ^+PH and O_2^+ required a resolving power of 3868, which was outside of the capabilities of the LNMS, and (C) the counts from ^+PH were potentially below the limit of detection when considering a ~15% yield, as per the NIST spectrum.

5. When considering deuterium isotopologues, and *only* exact mass, the mass at **35.005 amu** was consistent with $^+PH_2D$ as the dominant species given a Δamu = 0.001; with HDS^+ being a minor species due to a Δamu of 0.011 (which is outside the Δamu_{max}). Alternatively, the

counts of 12 at **35.005 amu** could represent the edge of a larger HDS^+ peak (34.993998 amu) – thus, implying higher actual counts for HDS^+ (and potentially a substantially higher D/H ratio). Or, the counts at **35.005 amu** could be mixed with $^{35}Cl^+$; though, $^{35}Cl^+$ and $^+PH_2D/HDS^+$ were likely sufficiently resolved (RP = 1061) and not substantially mixed.

6. In the main data table (**Table S2**), no other masses could be assigned to HDS; for example, the next closest value at **34.972 amu** was ill-matched due to a Δamu=0.022.

7. In the LNMS data, no other parent ions arising from neutral gases (beside PH_3^+), could account for atomic phosphorous. While alternative sources included H_3PO_3 (a neutral compound) or H_2PO_4 (an anion) at **81.975** and **96.667 amu**, these positions had counts of zero; which were interpreted, in this analysis, as counts <0.5. Therefore, fragmentation to yield atomic phosphorous in substantially higher relative yields (counts = 11) was considered highly unlikely. In support, insignificant yields for atomic sulfur were observed in the NIST reference spectrum for H_2SO_4 (≤1% of the parent ion; <0.5% of the base peak, SO_3^+). Note, reference spectra could not be found for phosphoric acid or phosphate. Due to an absence of fragmentation products (described in **Section 3.5**), H_3PO_3 and/or H_2PO_4 were not assigned.

8. In contrast, substantial counts were observed for sulfur-bearing species other than H_2S, such as H_xSO_y (counts of 3-15) and potentially elemental sulfur (counts of 128).

9. Together, these comparisons suggested that either (A) $^+PH_3$ and $^+PH_2$ were the predominant species at **33.992** and **32.985 amu**, or (B) that disentangling PH_3 and H_2S as parent gases was not possible.

These collective results are summarized in **Figures 1B-C**, which respectively display the measured LNMS masses, NIST reference spectra, and assignments using both PH_3 and H_2S. In summary, for PH_3, we find masses that correlate to P^+, $^+PH_2$, $^+PH_3$, and $^+PH_2D$, with the relative

intensities for P^+, $^+PH_2$, $^+PH_3$ following the same general trend as the reference spectrum. As mentioned previously, ^+PH was masked by O_2. Across the assignments, only $^+PH_3$ accounted for the presence of atomic phosphorous. In contrast, when considering H_2S, we find masses that correlate to S^+, ^+SH, and H_2S^+; while HDS^+ was outside of the Δamu_{max}, but not necessarily inconsistent with the assignment. Relative intensities of ^+SH and H_2S^+ followed the general trend of the reference, but atomic sulfur was enriched by ~1760% (when normalized to the base peak) – which was indicative of alternative sulfur sources, such as elemental sulfur. Regardless of assignment, fragmentation yields for $^+PH_3$ or H_2S^+ were higher than those in the NIST reference spectra, indicating enhanced loss of hydrogen. Moreover, the mass peaks at **34.005 amu** (counts = 21) and **33.992 amu** (counts = 19) were potentially mixed (RP = 2616); thereby casting additional uncertainty on the assignments. Given the similar counts at both positions, this composite mass potentially favored $^+PH_3$ over H_2S^+, or was a mixture containing $^+PH_3$ and $H_2O_2^+$ (Δamu = 0.001). Note, for $H_2O_2^+$, the fragmentation product of HO_2^+ (32.997825 amu) roughly correlated to the mass value of **32.985 amu** ($\Delta amu = 0.013 > \Delta amu_{max}$), which was assigned to $^+PH_2$ and/or HS^+, as detailed in step 3 above.

3.3 Ammonium

Mass data and assignments for ammonium (NH_4^+) and related fragments are provided in **Table S1**. As displayed in **Figure S1G**, the LNMS data show masses for NH_4^+, $^+NH_3$, $^+NH_2$, ^+NH, ^+N, with several species being enriched and/or mixed. We assigned the measured mass of **18.034 amu** as a composite consisting of NH_4^+ (Δamu = 0.000) with a fraction as $^+NH_2D$ (Δamu = 0.001), with the assumption of partial or sufficient resolution from H_2O. Similarly, we assigned the signal at **17.026 amu** as a composite mass consisting of $^+NH_3$ (Δamu = 0.001), ^+NHD (Δamu = 0.001) and $^{13}CH_4^+$ (Δamu = 0.009). We tentatively infer that the abundance of $^{13}CH_4^+$ is low due to the Δamu of 0.009 being greater than the Δamu_{max}. However, when considering the $^{13}C/^{12}C$ ratio (obtained from $^+CO_2$; Supplemental), calculation of expected $^{13}CH_4^+$ counts (from $^{12}CH_4^+$) exceeded those at the nearest mass position in the LNMS data. We've interpreted these results

as $^{13}CH_4^+$ being (A) the predominant species at **17.026 amu** or (B) co-mixed with non-negligible amounts of $^+NH_3$, which would require a lower $^{13}C/^{12}C$ ratio for CH_4.

Comparison of the NIST reference spectrum for NH_3 to the observed $^+N_xH_y$ fragments indicated substantial mixing and/or enrichment at the mass positions for $^+NH_2$ and ^+NH. For ^+NH (15.013 amu, measured), mixing with $^+CH_3$ (15.023 amu, measured) was a distinct possibility given that the 15 amu position was oversampled by the LNMS microprocessor. For $^+NH_2$, mixing with $^{12}CH_4^+$ was also possible given the high counts for $^{12}CH_4^+$ (39,936) and upper resolving power requirements (RP = 1233). However, when considering the mass signal for $^+NH_4$, alternative enrichment sources for $^+NH_2$ and ^+NH included ammonium-containing species such as salts.

3.4 Brønsted-Lowry Acids

Mass data and assignments for nitrous (HNO_2) and nitric (HNO_3) acids are provided in **Table S1**. In **Figure 1D**, the varying $H_xNO_y^+$ fragments are displayed against the mass spectrum for HNO_3 obtained from published reports (*Friedel et al.*, 1959; *O'Connor et al.*, 1997). For both acids we observe the parent ion (M^+), along with the fragments of HNO^+, NO^+, ^+OH, O^+, and N^+. Per our understanding, neither HNO_2^+ or HNO^+ are products of HNO_3^+ fragmentation. Hence, we interpret these masses as supporting the presence of both HNO_2 and HNO_3; with nitrous acid potentially being ~100-fold higher in abundance (assuming similar ionizing yields). Fragmentation of HNO_2 followed the same general trend as HNO_3 with apparent sequential loss of oxygen, hydrogen, and nitrogen. However, ^+OH was enriched, which is indicative of an alternative source, such as water. Despite correct mass values for both NO^+ (Δamu = 0.001) and NO_2^+ (Δamu = 0.002), which are both fragmentation products of HNO_3, these positions were respectively co-mixed with $C^{18}O$ and $C^{16}O^{18}O$. Adjustments of the counts using the $^{18}O/^{16}O$ ratio (Supplemental) provided estimates for NO^+ (but precluded NO_2).

Inspection of the mass values additionally revealed assignments for HCl and possibly HF, HCN, and $HClO_2$. Assignments are provided in **Table S1**, and plots against the NIST spectra for

HCl are provided in **Figure S1H**. Despite the potential for substantial mixing from $^{36}Ar^+$, fragmentation patterns for $H^{35}Cl$ and $H^{37}Cl$ tracked remarkably well with the NIST spectrum (thus, hinting at RP values of >1727 for the LNMS). For both HF and HCN, masses for both the M^+ and $[M-H]^+$ ions were components of unresolved mass pairs with $H_2{}^{18}O^+$ and $^{18}OH^+$, and $C_2H_3^+$ and $C_2H_2^+$, respectively. When compared to the NIST spectrum, the abundances of CN^+ were much higher than the reference, which supported mixing with $C_2H_2^+$ arising from ethane, ethene, or ethyne. For $HClO_2$, the mass at **50.969** amu was consistent with assignment of ClO^+ (Δamu = 0.005), while masses at **66.963** and **67.964 amu** were tentatively assigned as composites of ClO_2^+ (Δamu = 0.004) and $^{134}Xe^{2+}$, and $HClO_2^+$ (Δamu = 0.005) and $^{136}Xe^{2+}$, respectively. Thus, assignment of $HClO_2$ was considered tenuous due to significant overlap from xenon.

3.5 Oxysulfur Species and Sulfur

Mass data and assignments for fragments of sulfate ($H_xSO_y^+$) are provided in **Table S1**. In **Figure 1E**, the varying $H_xSO_y^+$ fragments are displayed against the NIST reference spectrum for H_2SO_4. In the LNMS data, no counts are observed for the parent ion of $H_2SO_4^+$ (M^+). However, a count of zero was recorded at a mass corresponding to the base peak of SO_3^+ ($[M-18]^+$). Surprisingly, we discovered several ensuing fragments for H_xSO_y with counts ranging from 2-10, including HSO_2^+ ($[M-33]^+$), SO_2^+ ($[M-34]^+$), HSO^+ ($[M-49]^+$), and SO^+ ($[M-50]^+$). Comparisons to the NIST spectrum show that fragmentation patterns (counts >0.5) follow the same general trend. However, the lack of gaseous parent ion for H_2SO_4 was perhaps suggestive of sulfate (SO_4^{2-}) or bisulfate (HSO_4^{1-}) being the parent species.

We also observe masses consistent with the isotopologues of $^{34}SO^+$, $H^{34}SO^+$, and $^{34}SO_2^+$. For $H^{34}SO^+$, and $^{34}SO_2^+$, the respective counts were disentangled using the $^{34}S/^{32}S$ ratio (Supplemental), which yielded expected counts of 0 and 1. For the assignment at **50.969 amu**, therefore, this suggested that $H^{34}SO^+$ was a trace species (at best), and that ClO (Δamu = 0.005) was the major species. Similarly, at **65.961 amu**, $^{34}SO_2^+$ was assigned as a minor species, with $^{132}Xe^{2+}$ being the likely major species. Similarly, $^{130}Xe^{2+}$ was likely mixed with HSO_2^+ at **64.960**

amu to yield a theoretical composite mass of 64.960825 amu (Δamu = 0.001), when considering equal abundance. In fact, the LNMS supported the presence of several Xe isotopes (^{124}Xe, ^{128}Xe, ^{129}Xe, ^{130}Xe, ^{132}Xe, and ^{134}Xe), with the collective Δamu values ranging from 0.000 to 0.018 – which was likely indicative of losses in resolving power at masses >120 amu.

Alternatively, hydrogen disulfide (H_2S_2) potentially served as a co-mixed species (Δamu = 0.001) at **65.961 amu**, along with $^{32}SO_2^+$ and/or $^{132}Xe^{2+}$. Relatedly, the mass for HS_2^+ (Δamu = 0.008), a fragment of H_2S_2, was also consistent with co-mixing at **64.960 amu** with HSO_2^+ and $^{130}Xe^{2+}$. While the notion of H_2S_2 (HS–SH) serving as an oxidized sink for H_2S is fascinating, we were unable to exclude $^{130}Xe^{2+}$ as the dominant species. Similarly, at the next mass position, HDS_2 was a good match (Δamu = 0.003), as was ClO_2 (Δamu = 0.004); however, the high counts of 280 at this position were suggestive of $^{134}Xe^{2+}$ being the dominant species. Likewise, at the following mass position, $HClO_2$ (Δamu = 0.003) was a good match; however, due to the high counts of 6272, $^{136}Xe^{2+}$ (an internal LNMS calibrant) was assigned as the dominant species. Interestingly, the ions of HPO_2^+ (Δamu = 0.010) and HPO^+ (Δamu = 0.011) potentially overlapped with SO_2^+ and SO^+; however, masses were attributed to $H_xSO_y^+$ due to assignment of $^{34}SO^+$, and similarity in fragmentation patterns between the LNMS and NIST data.

Lastly, estimated counts for atomic sulfur were ~30-fold higher than the next heaviest molecular sulfur species (SO^+), and ~18-fold higher than the assignment of H_2S^+, which was suggestive of enrichment from an alternative source. Given that O_2 and ^{32}S were likely poorly resolved, per *Hoffman et al.* (1980a) and our own measures, we estimated counts for ^{32}S using atomic ^{34}S and the $^{34}S/^{32}S$ ratio. As inferred from the $H_xSO_y^+$ fragments (counts and yields), sulfates/sulfuric acid were minimal contributors to atomic sulfur. Contributions from SO_2 were perhaps negligible, as SO_2^+ and SO^+ were also products of sulfuric acid degradation. Hence, we

posit that elemental sulfur (S_x) could be a major source of atomic sulfur, with the mass data showing possible evidence for a labile $^{+}S_5$ at **159.859 amu** (Δamu = 0.001).

4. Discussion

Our interpretation of the LNMS data supports the presence of minor species that potentially represent local disequilibria in the middle cloud layer. In reference to the pre-selected masses measured by the LNMS (*Hoffman et al.*, 1979a; *Hoffman et al.*, 1980a), we note that the actual pre-selected chemical identities are not available, and that many of the chosen mass pairs were at the edge or far beyond the resolving power of the LNMS. For this analysis, therefore, we conservatively approached the assignment of chemical identities to construct an internally consistent set of assignments where all parent ions were associated with fragmentation products, and all atomic CHNOPS elements were associated with parent ions.

For low-mass organics, the LNMS data support the presence of methane (CH_4), ethane (C_2H_6), benzene (C_6H_6), and possibly ethene (C_2H_4), ethyne (C_2H_2), and propyne (C_3H_4). While CH_4 and ^{136}Xe were used as an internal calibrants, *Donahue and Hodges* (1993) noted that respective levels for CH_4^+ (and associated fragments) increased, while those of $^{136}Xe^+$ remained constant, after opening of the gas inlets and during descent (prior to blockage of the gas inlets). These interpretations are suggestive of the presence of differing types of hydrocarbons in low-abundance in the middle clouds. When considering all carbon-containing parent species, our assignments support a range of carbon oxidation states including -4 (CH_4; C_2H_6), -3 (C_3H_4), -2 (C_2H_4), -1 (C_6H_6; possibly C_2H_2), 0 (C_3H_4), +2 (CO; possibly HCN), and +4 (CO_2).

When considering the legacy assignment of hydrogen sulfide (H_2S), our assessment of the data provides inconclusive evidence to support the presence of H_2S as the sole or dominant species. This assessment is perhaps similar to that of *Hoffman et al.* (1980a) who state that "there is strong, but presently inconclusive, evidence for H_2S." Rather, in our model, phosphine (PH_3) seems to better fit the total mass data since no other phosphorous-containing parent gases could be assigned to atomic phosphorous. However, unambiguous assignment of PH_3 or

H_2S was not possible, as the required resolving power was certainly outside of the capabilities of the LNMS. For atomic sulfur, our assignments were suggestive of elemental sulfur being the dominant parent species.

When considering deuterium isotopologues, a ratio of ~$6x10^{-1}$ was obtained for PH_2D/PH_3 or HDS/H_2S at an altitude of 51.3 km. This value was substantially higher than the ratios for HDS/H_2S ($5x10^{-2}$), HDO/H_2O ($5x10^{-2}$), and CH_3D/CH_4 ($5x10^{-3}$) reported by *Donahue and Hodges* (1993), which (per our understanding) represent averages across the atmosphere. Given our identical mass assignments for HDS and H_2S, the high ratio obtained at 51.3 km was possibly indicative of statistical variation in the counts. In addition, we note that PH_3 and H_2S exhibit similar degrees of hydrogen-deuterium exchange (*Jones and Sherman*, 1937; *Weston Jr. and Bigeleisen*, 1952; *Wada and Kiser*, 1964; *Fernández-Sánchez and Murphy*, 1992).

The LNMS data also show evidence for several acidic species including ammonium (NH_4^+), nitrous acid (HNO_2), nitric acid (HNO_3), hydrochloric acid ($H^{37}Cl$ & $H^{35}Cl$), and possibly hydrofluoric acid (HF), chlorous acid ($HClO_2$), and hydrogen cyanide (HCN). As displayed in **Figure 1F**, the combined data for NH_4^+ and the H_xSO_y fragments show considerable similarity to the mass spectra for $(NH_4^+)_2SO_4$ (*Dovrou et al.*, 2019). This comparison opens the suggestion that ammonium sulfate ($(NH_4^+)_2SO_4$) may be an atmospheric component, either as an aqueous aerosol species or nanoparticle. In the data, consideration of all nitrogen-containing parent species (including conjugate bases) supported oxidation states of -3 (NH_4^+, and possibly NH_3 and ^-CN), 0 (N_2), +3 (NO_2^-), and +5 (NO_3^-).

The LNMS data additionally support the presence of O_2, CO, and possibly COS and NSCl. While parent ions of COS and NSCl are observed, no fragmentation products could be identified, other than the atomic elements. For CO, comparison of the CO_2 fragmentation patterns revealed higher CO^+/CO_2^+ ratios in the LMNS data (~0.3) when compared to the NIST reference (~0.1), which was indicative of higher amounts of CO^+ in the Venus sample. In control experiments, however, *Hoffman et al.* (1979b) observed a CO^+/CO_2^+ ratio of ~0.4 when the gate

valve to the ion source in the LMNS was closed. At an altitude of 51.3 km (~ 1 bar), therefore, we presume that the gate valve was partially open. These assumptions, therefore, support the presence of CO as an atmospheric component. Lastly, the data support the presence of oxygen gas (O_2), which *Hoffman et al.* (1980a) attribute to dissociative ionization of CO_2 and SO_2. However, the NIST reference spectra for CO_2 (**Figure 1A**) and SO_2 (*Wallace*, 2020) show no formation of O_2 despite equivalent impact energies. We posit, therefore, that O_2 may be a minor atmospheric constituent at 51.3 km.

Conclusion

Our interpretations of the LNMS data illuminate the potential for disequilibria within the clouds. In fact, disequilibria was discussed by *Florenskii et al.* (1978), regarding Venera 8 observations of NH_3 (*Surkov et al.*, 1973), and by *Zolotov* (1991) regarding the lower atmosphere. If correct, this suggests that disparate chemicals across varying oxidation states are sustained by unknown chemistries. We speculate that this includes the generation of appreciable reducing power through volcanism or other geochemical inputs (*e.g. Ivanov and Head* (2013); *Shalygin et al.* (2015); *Gülcher et al.* (2020)). In summary, our interpretations hint at the clouds (at 51.3 km) containing minor abundances of low-mass organics, Brønsted-Lowry acids, and reduced main group molecules including nitrite, elemental sulfur, methane, ethane, and phosphine and/or hydrogen sulfide.

Interestingly, when considering the hypothetical habitability of Venus' clouds, our assignments reveal a potential electron donor for anoxygenic photosynthesis (nitrite) (*Griffin et al.*, 2007), and all major constituents of the nitrogen cycle (nitrate, nitrite, possibly ammonium, and N_2) (*Madigan et al.*, 2014). Further, *Limaye et al.* (2018) suggested that the nitrate/nitrite redox pair may couple to a postulated iron-sulfur biogeochemical cycle in Venus' clouds. Lastly, our interpretations suggest that phosphine may be present in the clouds; though any potential mixtures with hydrogen sulfide could not be disambiguated. Looking ahead, these analyses

support continued study of the recently released PV LNMS archive data, including new measurements.

Statement of Contributions

All authors (RM, SSL, & MJW) contributed to analysis of the data, assisted in drafting of the report, approved of the submission, and agreed to be accountable for the respective contributions. RM is the corresponding author.

Acknowledgments, Samples, and Data

Acknowledgements

We acknowledge Jaime A. Cordova, Jr. for insightful assistance with chemical assignments and manuscript preparation. RM acknowledges support from the National Aeronautics and Space Administration (NASA) Research Opportunities in Space and Earth Sciences (NNH18ZDA001N). SSL was supported by NASA (NNX16AC79G). MJW was supported by the NASA Astrobiology Program through collaborations arising from his participation in the Nexus for Exoplanet System Science (NExSS) and the NASA Habitable Worlds Program. MJW also acknowledges support from the GSFC Sellers Exoplanet Environments Collaboration (SEEC), which is funded by the NASA Planetary Science Division's Internal Scientist Funding Model.

Data Availability

All LNMS data used in this study were obtained from published reports (*Hoffman et al.*, 1980a; *Hoffman et al.*, 1980b). The LNMS archive data were also posted online on October 8, 2020 by the NASA Space Science Data Coordinated Archive (NSSDC) (https://nssdc.gsfc.nasa.gov/nmc/dataset/display.action?id=PSPA-00649).

Statement of Conflict of Interest

All authors declare no conflict of interest.

References

Donahue, T., J. Hoffman, and R. Hodges Jr (1981), Krypton and xenon in the atmosphere of Venus, *Geophysical Research Letters*, *8*(5), 513-516.

Donahue, T. M., and R. R. Hodges (1993), Venus methane and water, *Geophysical Research Letters*, *20*(7), 591-594.

Donahue, T. M., and R. R. Hodges, Jr. (1992), Past and present water budget of Venus, *Journal of Geophysical Research*, *97*, 6083-6091.

Donahue, T. M., J. H. Hoffman, R. R. Hodges, and A. J. Watson (1982), Venus was wet - A measurement of the ratio of deuterium to hydrogen, *Science*, *216*, 630-633.

Dovrou, E., C. Y.-T. Lim, M. R. Canagaratna, J. Kroll, D. R. Worsnop, and F. N. Keutsch (2019), Measurement techniques for identifying and quantifying hydroxymethanesulfonate (HMS) in an aqueous matrix and particulate matter using aerosol mass spectrometry and ion chromatography.

Fernández-Sánchez, J., and W. Murphy (1992), Raman scattering cross sections and polarizability derivatives of H_2S, D_2S, and HDS, *Journal of Molecular Spectroscopy*, *156*(2), 431-443.

Florenskii, C. P., V. P. Volkov, and O. V. Nikolaeva (1978), A geochemical model of the Venus troposphere, *Icarus*, *33*, 537.

Friedel, R. A., J. L. Shultz, and A. G. Sharkey (1959), Mass spectrum of nitric acid, *Analytical Chemistry*, *31*(6), 1128-1128.

Greaves, J. S., A. M. Richards, W. Bains, P. B. Rimmer, H. Sagawa, D. L. Clements, S. Seager, J. J. Petkowski, C. Sousa-Silva, and S. Ranjan (2020), Phosphine gas in the cloud decks of Venus, *Nature Astronomy*, 1-10.

Griffin, B. M., J. Schott, and B. Schink (2007), Nitrite, an electron donor for anoxygenic photosynthesis, *Science*, *316*(5833), 1870-1870.

Gülcher, A. J. P., T. V. Gerya, L. G. J. Montési, and J. Munch (2020), Corona structures driven by plume–lithosphere interactions and evidence for ongoing plume activity on Venus, *Nature Geoscience*.

Haynes, W. M. (Ed.) (2016), *CRC Handbook of Chemistry and Physics*, 97th Edition ed., 1-12 pp., CRC Press, Boca Raton, Florida.

Hoffman, J. H., R. R. Hodges, T. M. Donahue, and M. B. McElroy (1980a), Composition of the Venus lower atmosphere from the Pioneer Venus mass spectrometer, *Journal of Geophysical Research: Space Physics*, *85*(A13), 7882-7890.

Hoffman, J. H., R. R. Hodges, and K. D. Duerksen (1979a), Pioneer Venus large probe neutral mass spectrometer, *Journal of Vacuum Science and Technology*, *16*(2), 692-694.

Hoffman, J. H., R. R. Hodges, M. B. McElroy, T. M. Donahue, and M. Kolpin (1979b), Composition and structure of the Venus atmosphere: Results from Pioneer Venus, *Science*, *205*(4401), 49-52.

Hoffman, J. H., R. R. Hodges, M. B. McElroy, T. M. Donahue, and M. Kolpin (1979c), Venus lower atmospheric composition: Preliminary results from Pioneer Venus, *Science*, *203*(4382), 800-802.

Hoffman, J. H., R. R. Hodges, W. W. Wright, V. A. Blevins, K. D. Duerksen, and L. D. Brooks (1980b), Pioneer Venus sounder probe neutral gas mass spectrometer, *IEEE Transactions on Geoscience and Remote Sensing*(1), 80-84.

Hoffman, J. H., V. I. Oyama, and U. Von Zahn (1980c), Measurements of the Venus lower atmosphere composition: A comparison of results, *Journal of Geophysical Research: Space Physics*, *85*(A13), 7871-7881.

Ivanov, M. A., and J. W. Head (2013), The history of volcanism on Venus, *Planetary and Space Science*, *84*, 66-92.

Johnson, N. M., and M. R. de Oliveira (2019), Venus atmospheric composition in situ data: a compilation, *Earth and Space Science*, *6*(7), 1299-1318.

Jones, T., and A. Sherman (1937), Calculation of Equilibrium Constants and Activation Energies for Some Reactions Involving Various Isotopic Species of Hydrogen, Water, and Hydrogen Sulfide, *The Journal of Chemical Physics*, *5*(6), 375-381.

Kliore, A. J., V. I. Moroz, and G. Keating (1985), The Venus International Reference Atmosphere, *Advances in space research*, *5*(11), 8-305.

Kumar, S., D. M. Hunten, and H. A. Taylor Jr (1981), H_2 abundance in the atmosphere of Venus, *Geophysical Research Letters*, *8*(3), 237-240.

Limaye, S. S., R. Mogul, D. J. Smith, A. H. Ansari, G. P. Słowik, and P. Vaishampayan (2018), Venus' Spectral Signatures and the Potential for Life in the Clouds, *Astrobiology*, *18*(9), 1181-1198.

Madigan, M. T., J. M. Martinko, K. S. Bender, D. H. Buckley, and D. A. Stahl (2014), *Brock Biology of Microorganisms*, Pearson, New York, NY.

Moroz, V. (1981), The atmosphere of Venus, *Space Science Reviews*, *29*(1), 3-127.
O'Connor, C. S., N. C. Jones, and S. D. Price (1997), Electron-impact ionization of nitric acid, *International journal of mass spectrometry and ion processes*, *163*(1-2), 131-139.
Oyama, V. I., G. C. Carle, F. Woeller, J. B. Pollack, R. T. Reynolds, and R. A. Craig (1980), Pioneer Venus gas chromatography of the lower atmosphere of Venus, *Journal of Geophysical Research*, *85*, 7891-7902.
Pollack, J. B., J. B. Dalton, D. Grinspoon, R. B. Wattson, R. Freedman, D. Crisp, D. A. Allen, B. Bezard, C. DeBergh, and L. P. Giver (1993), Near-infrared light from Venus' nightside: A spectroscopic analysis, *Icarus*, *103*(1), 1-42.
Seager, S., J. J. Petkowski, P. Gao, W. Bains, N. C. Bryan, S. Ranjan, and J. Greaves (2020), The Venusian lower atmosphere haze as a depot for desiccated microbial life: A proposed life cycle for persistence of the Venusian aerial biosphere, *Astrobiology*, *Online Ahead of Print: August 13, 2020*.
Shalygin, E. V., W. J. Markiewicz, A. T. Basilevsky, D. V. Titov, N. I. Ignatiev, and J. W. Head (2015), Active volcanism on Venus in the Ganiki Chasma rift zone, *Geophysical Research Letters*, *42*(12), 4762-4769.
Smirnova, T., and A. Kuz'min (1974), Water-vapor and ammonia abundance in the lower atmosphere of Venus estimated from radar measurements, *Soviet Astronomy*, *18*, 357.
Surkov, I. A. (1977), Geochemical studies of Venus by Venera 9 and 10 automatic interplanetary stations, paper presented at Lunar and Planetary Science Conference Proceedings, Houston, TX, March 14-18, 1977.
Surkov, Y. A., B. M. Andrejchikov, and O. M. Kalinkina (1973), On the content of ammonia in the Venus atmosphere based on data obtained from Venera 8 automatic station, *Akademiia Nauk SSSR Doklady*, *213*, 296.
Von Zahn, U., and V. Moroz (1985), Composition of the Venus atmosphere below 100 km altitude, *Advances in space research*, *5*(11), 173-195.
Wada, Y., and R. W. Kiser (1964), Mass Spectrometric Study of Phosphine and Diphosphine, *Inorganic Chemistry*, *3*(2), 174-177.
Wallace, W. E. (2020), "Mass Spectra" in NIST Chemistry WebBook, NIST Standard Reference Database Number 69, edited by P. J. L. a. W. G. Mallard, National Institute of Standards and Technology, Gaithersburg MD, 20899.
Weston Jr., R. E., and J. Bigeleisen (1952), Equilibrium in the Exchange of Hydrogen between Phosphine and Water, *The Journal of Chemical Physics*, *20*(9), 1400-1402.
Zolotov, M. Y. (1991), Redox Conditions of the Near Surface Atmosphere of Venus. II. Equilibrium and Disequilibrium Models, edited, p. 1573.